

Supporting Information to Accompany:

A Pendant Proton Shuttle on $[\text{Fe}_4\text{N}(\text{CO})_{12}]^-$ Provides Further Insight for a Reduced Hydride as Catalytic Intermediate

Natalia D. Loewen, Emily J. Thompson, Michael Kagan, Carolina L. Banales, Thomas W. Myers, James C. Fettinger, and Louise A. Berben*

Department of Chemistry, University of California, Davis, CA 95616

email to: laberben@ucdavis.edu

Table S1. Crystallographic data for and $[\text{Et}_4\text{N}][\text{Fe}_4(\text{N})(\text{CO})_{11}\text{PPh}_3]$ (**Et₄N-1**) and $[\text{Et}_4\text{N}][\text{Fe}_4(\text{N})(\text{CO})_{11}\text{PPh}_2\text{EtOH}]$ (**Et₄N-2**).

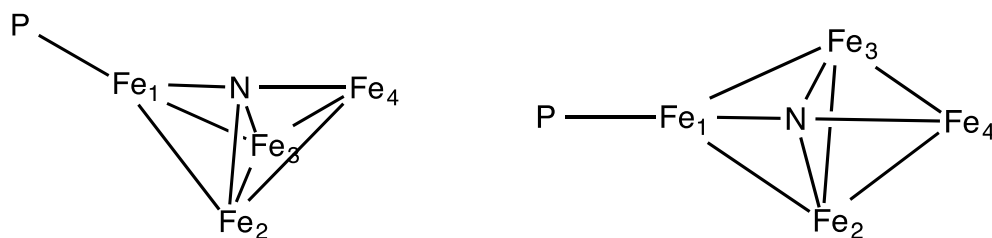
	Et ₄ N-1•C ₄ H ₈ O	Et ₄ N-2
Formula	C ₃₃ H ₃₅ Fe ₄ N ₂ O ₁₂ P, C ₄ H ₈ O	C ₃₃ H ₃₅ Fe ₄ N ₂ O ₁₂ P
Crystal size	0.37 × 0.33 × 0.29	0.18 × 0.21 × 0.43
Formula weight, g mol ⁻¹	1010.14	906.00
Space group	<i>I</i> 2/ <i>a</i>	<i>P</i> 2 ₁ / <i>c</i>
<i>a</i> , Å	25.630(2)	18.495(3)
<i>b</i> , Å	10.6233(8)	10.4499(15)
<i>c</i> , Å	31.622(2)	20.683(3)
<i>α</i> , deg	90	90
<i>β</i> , deg	95.408(1)	112.149(2)
<i>γ</i> , deg	90	90
<i>V</i> , Å ³	8571.4(11)	3702.6(9)
<i>Z</i>	8	4
<i>T</i> , K	90 (2)	90 (2)
<i>ρ</i> , calcd, g cm ⁻³	1.566	1.625
Refl. collected/2 θ_{max}	37485/55.77	38711/54.99
Unique refl./ <i>I</i> > 2 σ (<i>I</i>)	10203/9215	8506/7559
No. parameters/restrains	595/8	511/1
λ , Å/ μ (K α), cm ⁻¹	0.71073	0.71073
R ₁ /GOF	0.0229/1.056	0.0240/1.030
wR ₂ (<i>I</i> > 2 σ (<i>I</i>)) ^a	0.0572	0.0594
Residual density, e Å ⁻³	+0.461/-0.214	+0.601/-0.307

$$^a R_1 = \frac{\sum ||F_o| - F_c||}{\sum |F_o|}, wR_2 = \left\{ \frac{\sum [w(F_o^2 - F_c^2)^2]}{\sum [w(F_o^2)^2]} \right\}^{0.5}.$$

Table S2. Selected average interatomic distances (Å) and selected average angles (deg) for [Et₄N][Fe₄(N)(CO)₁₁PPh₃] (Et₄N-1), [Et₄N][Fe₄(N)(CO)₁₁PPh₂EtOH] (Et₄N-2), and previously reported [Et₄N][Fe₄(N)(CO)₁₂].¹ See Chart S1 for atom numbering scheme.

	Et ₄ N-1•C ₄ H ₈ O	Et ₄ N-2	[Et ₄ N][Fe ₄ (N)(CO) ₁₂]
Fe ₁ -N	1.768(1)	1.771(2)	1.768(3)
Fe ₂ -N	1.891(1)	1.915(1)	1.896(3)
Fe ₃ -N	1.923(1)	1.905(1)	1.909(3)
Fe ₄ -N	1.781(1)	1.789(2)	1.775(3)
Fe ₁ -Fe ₂	2.6569(7)	2.6529(5)	2.6186(7)
Fe ₁ -Fe ₃	2.6113(8)	2.5902(4)	2.6005(7)
Fe ₂ -Fe ₃	2.5029(8)	2.4790(5)	2.5065(7)
Fe ₂ -Fe ₄	2.5897(8)	2.5817(6)	2.6147(7)
Fe ₃ -Fe ₄	2.5943(6)	2.5961(7)	2.5916(7)
Fe ₁ -P	2.2206(6)	2.2028(6)	--
Fe ₂ -Fe ₁ -Fe ₃	56.72(2)	56.87(1)	57.40(2)
Fe ₁ -Fe ₂ -Fe ₄	85.09(2)	85.67(1)	85.19(2)
Fe ₁ -Fe ₃ -Fe ₄	85.93(2)	86.67(1)	86.02(2)

Chart S1. Atom numbering scheme for Table S2.



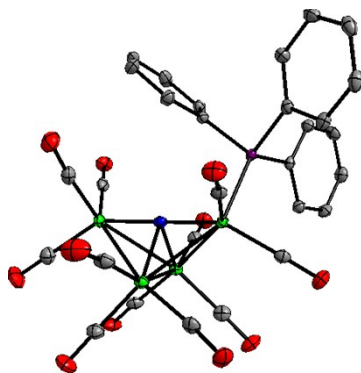


Figure S1. Solid state structure of $[\text{Fe}_4(\text{N})(\text{CO})_{11}\text{PPh}_3]^-$ in $\text{Et}_4\text{N}-\mathbf{1}$. Green, grey, blue, pink and red atoms represent Fe, C, N, P and O atoms, respectively. Ellipsoids are shown at 50 % probability. H atoms, counter cation, and solvent molecule are omitted for clarity.

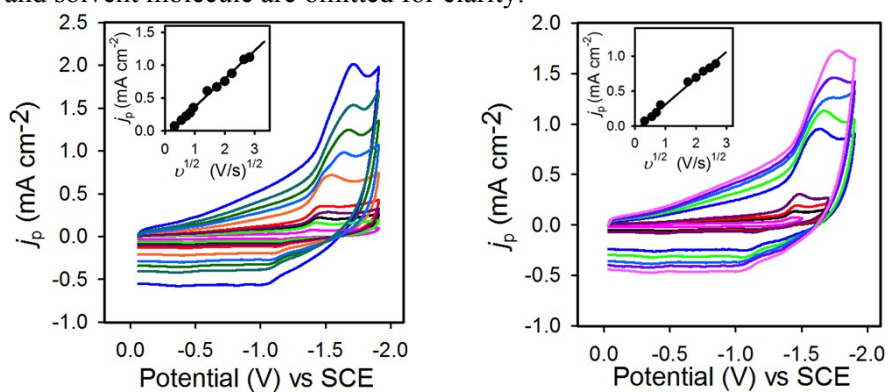


Figure S2. CVs of (left) $\mathbf{1}^-$ and (right) $\mathbf{2}^-$ at different scan rates. Inset: j_p vs. $v^{1/2}$. Black line is linear fit to the data. 0.1 M Bu_4NPF_6 MeCN solution, glassy carbon working electrode.

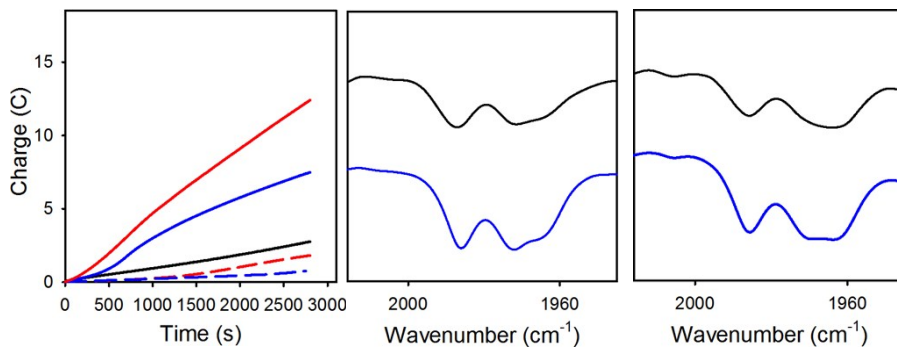


Figure S3. (Left) Plot of charge vs. time in a representative CPE experiment with 0.1 mM $\mathbf{1}^-$ (solid blue), and with 0.1 mM $\mathbf{2}^-$ (solid red). CPE experiments were rerun using the uncleaned working electrode in fresh electrolyte solution to check for deposited catalyst: $\mathbf{1}^-$ (dashed blue), and $\mathbf{2}^-$ (dashed red), CPE run with no catalyst (black). Glassy carbon working electrode, 0.1 M Bu_4NPF_6 in MeCN/ H_2O (95:5), -1.40 V vs SCE, 1 atm CO_2 . (middle) IR spectra of the CPE solution before (blue) and after (black) a CPE experiment with $\mathbf{1}^-$. (right) IR spectra of the CPE solution before (blue) and after (black) an experiment with $\mathbf{2}^-$.

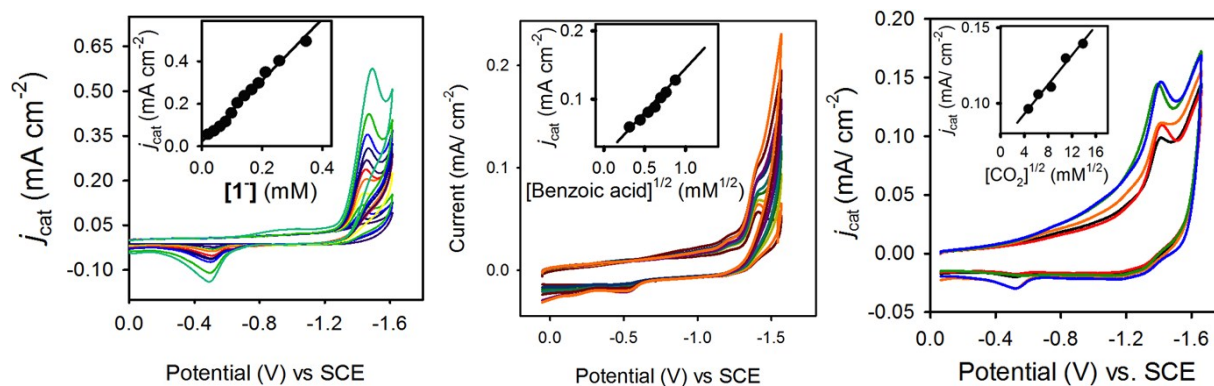


Figure S4. (left) CV's recorded in 0.1 M Bu_4NPF_6 MeCN/ H_2O (95:5) solution with added aliquots of $\mathbf{1}^-$, under 1 atm CO_2 . Inset: plot of j_{cat} vs. $[\mathbf{1}^-]$ at -1.45 V vs. SCE. (middle) CV's recorded in 0.1 M Bu_4NPF_6 MeCN solution with 0.1 mM $\mathbf{1}^-$ and added aliquots of H^+ , under 1 atm CO_2 . Inset: plot of j_{cat} vs. $[\text{H}^+]^{1/2}$ at -1.45 V vs. SCE. (right) CV's recorded in 0.1 M Bu_4NPF_6 MeCN/ H_2O (95:5) solution with 0.1 mM $\mathbf{1}^-$, and added aliquots of CO_2 . Inset: plot of j_{cat} vs. $[\text{CO}_2]^{1/2}$ at -1.45 V vs. SCE.

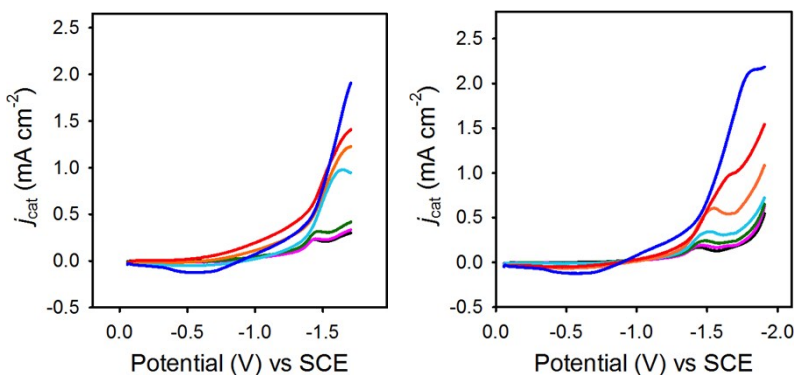


Figure S5. Background subtracted CV's showing the scan rate independence of $\mathbf{1}^-$ (left) under 1 atm CO_2 , recorded from 0.5 to 6 Vs^{-1} , and (right) under 1 atm N_2 , recorded from 0.3 to 7 Vs^{-1} . The scan rate independent region was used to calculate rate constants along with equation 2 (see main text).

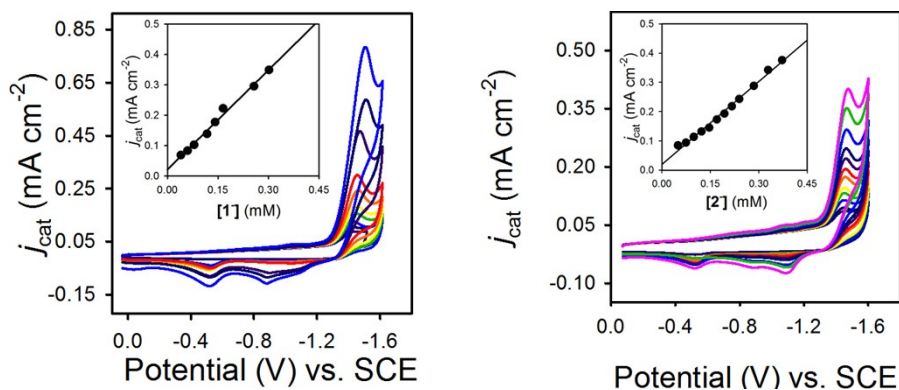


Figure S6. CV's recorded in 0.1 M Bu₄NPF₆ MeCN/H₂O (95:5) solution under 1 atm N₂. (left) with added aliquots of **1**⁻, and (right) with added aliquots of **2**⁻. Insets: j_{cat} vs. [**1**⁻] at -1.45 V vs. SCE (left), and j_{cat} vs. [**2**⁻] at -1.47 V vs. SCE (right). This shows that the reaction is first order with respect catalyst in each case.

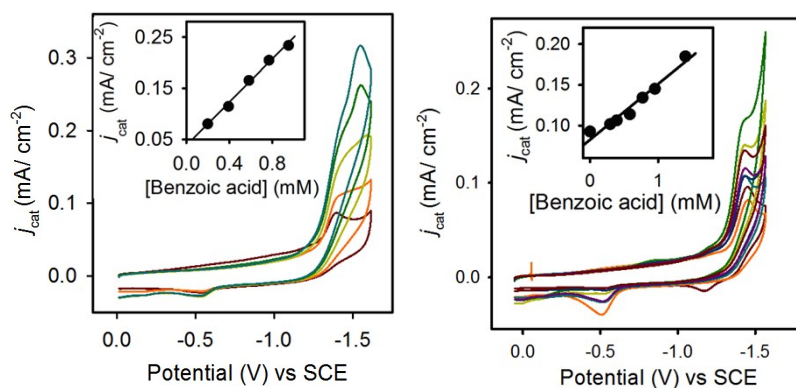


Figure S7. CV's recorded in 0.1 M Bu₄NPF₆ MeCN solution under 1 atm N₂ with various amounts of benzoic acid, and (left) 0.1 mM **1**⁻; (right) 0.1 mM **2**⁻. Insets: plot of j_{cat} vs. [H⁺] at -1.45 V (left), and at -1.47 V (right) vs. SCE. This indicates that each reaction is second order in [H⁺].

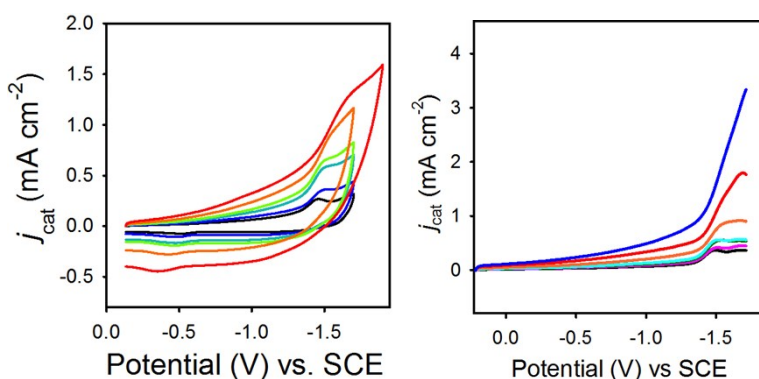


Figure S8. (Left) CV's recorded in 0.1 M Bu₄NPF₆ MeCN/H₂O (95:5) with varied scan rates for 0.1 mM **2**⁻ under 1 atm N₂. (Right) Background corrected CV's from 0.5 to 6 Vs⁻¹, showing scan rate independence between 0.5 and 1 Vs⁻¹.

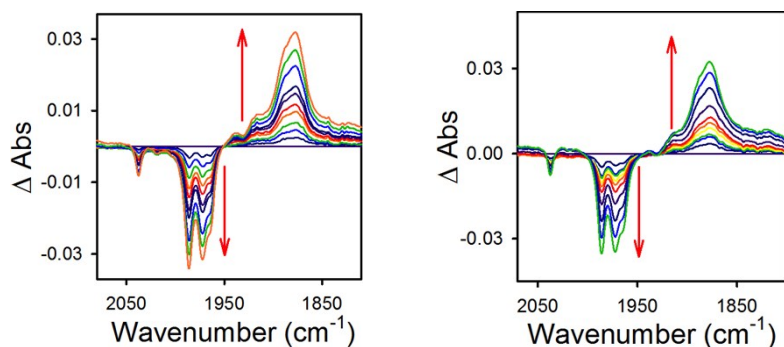


Figure S9. (Left) IR-SEC experiment showing differential absorbance spectra for reduction of $\mathbf{1}^-$ at -1.45 V vs. SCE in the presence of 10 equivalents (3 mM) of benzenesulfonamide acid. The features are the same as those observed when the cluster is reduced in rigorously dried acetonitrile, and suggest that no formation of ($\mathbf{H-1}^-$) occurs. (Right) IR-SEC experiment showing differential absorbance spectra for reduction of $\mathbf{1}^-$ at -1.45 V vs. SCE in presence of 10 equivalents (3 mM) of butyric acid.

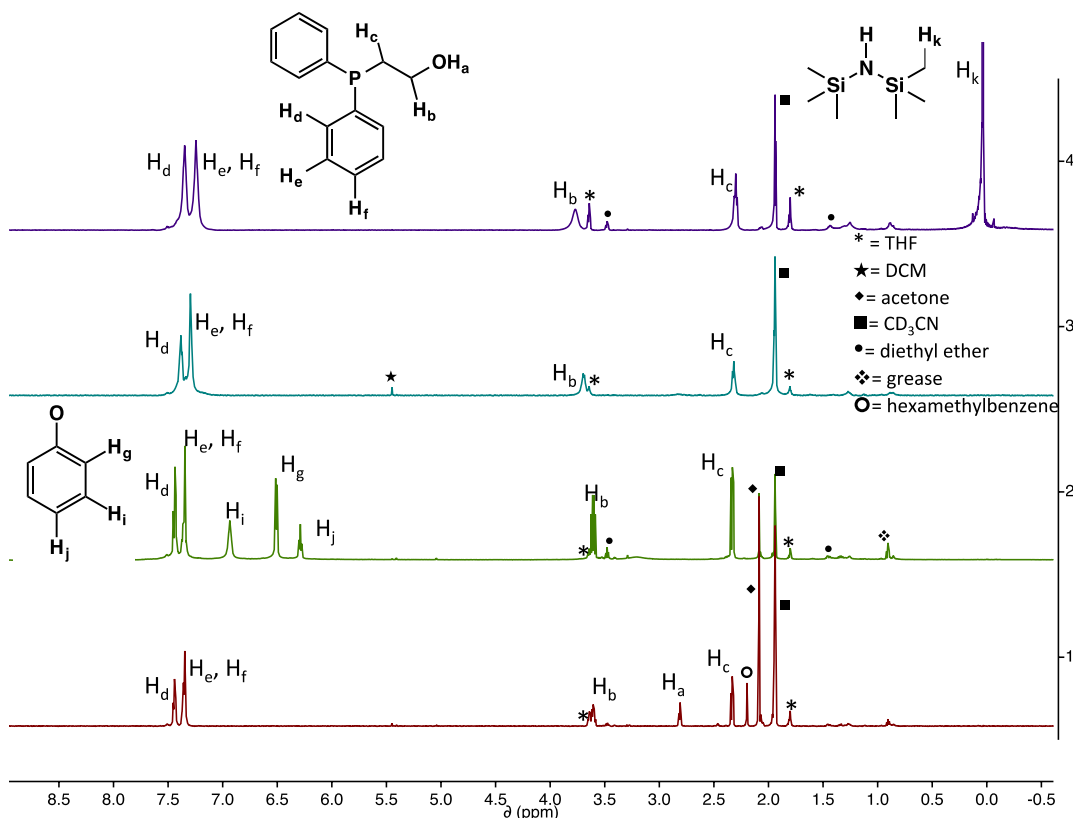


Figure S10. ^1H NMR spectra of CD_3CN solutions of (red) $\text{P}(\text{Ph})_2(\text{CH}_2)_2\text{OH}$, (green) a mixture of $\text{P}(\text{Ph})_2(\text{CH}_2)_2\text{OH}$ and NaOPh , (blue) $\text{P}(\text{Ph})_2(\text{CH}_2)_2\text{OLi}$, and (purple) a mixture of $\text{P}(\text{Ph})_2(\text{CH}_2)_2\text{OH}$ and NaHMDS . The purple spectrum shows the H_c peak shift downfield after deprotonation by NaHMDS , along with slight shifts in the phenyl region. The lack of a similar shift in the green spectrum suggests that no deprotonation has occurred using NaOPh . We attribute the disappearance of the sharp H_a peak, along with the presence of a very broad resonance in the baseline at 3.25 ppm, to hydrogen bonding with the phenoxide anion.

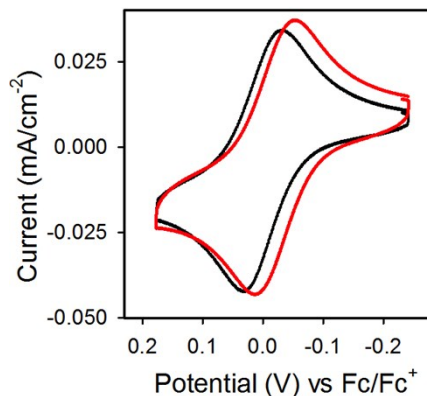


Figure S11. CV scans showing the ferrocene/ferrocenium redox couple in: (black) 0.1 M Bu_4NPF_6 MeCN and (red) 95:5 mixture of MeCN/ H_2O with 0.1 M Bu_4NPF_6 . Both scans are referenced to the $E_{1/2}$ for Fc/Fc^+ (black), using the same reference electrode. The cathodic shift of the red trace is 18 mV.

Correcting for effects of homoconjugation. Homoconjugation effects would be quantifiable based on the equation shown below.

$$\kappa = K_c C_0$$

Here, κ is a dimensionless parameter, K_c is the homoconjugation equilibrium constant for the reaction $\text{HA} + \text{A}^- \leftrightarrow \text{AHA}^-$ where HA is acid and A^- is the conjugate base and C_0 is the bulk concentration of acid. If κ is greater than 1, homoconjugation should be taken into account. Acid concentrations employed in $\text{p}K_a$ and hydricity measurements in IR-SEC experiments always fell between 0.3 and 3.0 mM, and using K_c values reported by Artero and coworkers at these concentrations homoconjugation effects are negligible.²

¹ M. D. Rail, L. A. Berben, *J. Am. Chem. Soc.*, 2011, **133**, 18577.

² V. Fourmond, P.-A. Jacques, M. Fontecave, V. Artero, *Inorg. Chem.*, 2010, **49**, 10338.